

<https://doi.org/10.52676/1729-7885-2023-2-66-73>

УДК 538.915

FIRST-PRINCIPLES STUDIES OF $X_2\text{FeSi}$ HEUSLER ALLOYS

N. A. Merali¹, N. S. Soltanbek¹, F. U. Abuova¹, T. M. Inerbaev^{1,2}, S. A. Nurkenov^{1,3}, A. U. Abuova^{1*}

¹ L.N. Gumilyov Eurasian National University, Astana, Kazakhstan

² Sobolev Institute of Geology and Mineralogy, Novosibirsk, Russia

³ Astana International University, Astana, Kazakhstan

* E-mail for contacts: aisulu-us1980@yandex.kz

The characteristics related to electricity and magnetism in Heusler alloys with both full ($L2_1$) and inverse (XA) structures $X_2\text{FeSi}$ ($X = \text{Mn}, \text{V}$) have been studied within the framework of the Density Functional Theory. Three different methods, namely LDA, GGA, and SCAN, were used to perform calculations. The aim was to investigate the energy stability of the $L2_1$ and XA structures for these compositions. The findings revealed that the XA structure is energetically stable for both structures. The choice of functional is indicated does not have a qualitative effect on the energy stability of the phases. Based on calculations, it was found that meta-GGA (SCAN) more accurately describes the electronic properties of these alloys. In the process of the calculations, it was found that these compounds are semimetals. An analysis was conducted from a local environment perspective to investigate and understand the reasons behind the semi-metallic band gap and the variations in electronic and magnetic properties observed in Heusler compounds. Calculations also showed that the magnetic moment Mn_2FeSi for both structures was $1.99 \mu_B/\text{f.u.}$ With regard to V_2FeSi , $\mu = 2.00 \mu_B/\text{f.u.}$ for structure XA and $\mu = 2.37 \mu_B/\text{f.u.}$ for structure $L2_1$. These calculations are consistent with the Slater-Pauling rule for the XA structure.

Keywords: Heusler alloys, DFT study, magnetic properties.

INTRODUCTION

Heusler compounds with a face centered cubic (fcc) structure attract much attention is paid because of their possible use in microelectronics and spintronics. Certain Heusler compounds exhibit high structural stability and 100% spin polarization, and are classified as semimetals [1]. Previous studies have investigated the electronic, magnetic, and structural properties of various Heusler compounds using both first-principle calculations based on DFT (Density Functional Theory) and experimental methods. These studies are cited in references [2–8]. Heusler alloys crystallize in two possible structures: $L2_1$ (spatial symmetry group $\text{Fm}\bar{3}\text{m}$) and XA (spatial symmetry group $\text{F}\bar{4}3\text{m}$). Interest in these compounds is not least because of the fact that the properties of complete Heusler alloys strongly depend on their structure and composition. Mn_2FeX ($X = \text{Al}, \text{Si}$) compounds in $L2_1$, XA structures were studied by DFT + GGA methods in a number of works [9, 10].

The cubic phase of Mn_2FeSi was synthesized by annealing [11–13]. It is shown that Mn_2FeSi crystallizes into an inverse XA structure. Recent works [7, 14] also report that Mn_2FeSi adopts a cubic inverse-heusler (XA) structure. Calculations with Density Functional Theory [9–11] have shown that the XA structure of Mn_2FeSi is a semimetal with a total magnetic moment of $2 \mu_B$. Thus, it is assumed that Heusler compounds with transition metals can exhibit special properties, such as semimetallicity, both in the $L2_1$ structure and in the XA structure, depending on the chemical structure.

In the work [15] explains the appearance of semimetallic properties of Mn_2FeSi (XA, $L2_1$ structures) with the behavior of t_{2g} electrons of transition metal

atoms, where the delocalization of these electrons leads to a strong decrease in the semimetallic band gap.

Recent X-ray diffraction analyses were conducted on Mn_2FeSi , a triple Heusler alloy that was synthesized. The results revealed that, at room temperature, the prepared samples had an uneven magnetic structure characterized by a dominance of paramagnetic phases, and a minor ferro/ferrimagnetic contribution was identified along the magnetization curves [16].

The compositional dependences from magnetic exchange interactions for the cubic phase $\text{Fe}_{2+x}\text{Mn}_{1-x}\text{Al}$ Heusler alloy, where $0.0 < x < 1.0$, were obtained by first-principles calculations and demonstrated that nearest neighbors of Fe-Fe represent a strong ferromagnetic bond [17].

In the literature [18], it was presented that the replacement of Mn by Fe in Heusler alloys ($\text{Mn}_{1-x}\text{Fe}_x$) $_2\text{VSi}$ at a concentration of $x = 0.5$ become semimetals and, consequently, non-magnetic.

Existing studies give an idea of the useful properties and prospects of Mn_2FeSi Heusler alloys [7, 8]. However, in such studies, only one of the possible structures of Heusler alloys was mainly considered. Comparing the characteristics of certain Heusler alloys in both $L2_1$ and XA structures is important. Thus, the aim of this study is to conduct a comparative analysis of Mn_2FeSi and V_2FeSi Heusler compounds in both inverse (XA) and full ($L2_1$) structures to identify the factors responsible for the formation of diverse magnetic, structural, and electronic properties. Additionally, the study will explore the impact of three different functionals, namely LDA, GGA, and meta-GGA, on the properties of Heusler alloys.

METHODOLOGY

Density functional calculations of the electronic structure were performed using the VASP program code, employing a plane wave basis. The method of projection attached waves (projector augmented wave – PAW) was used [19]. The LDA [20, 21], the GGA in the case of the PBE [22], and the SCAN [23] meta-GGA [24] are used for comparative studies. In the calculations for all cases, the cutoff of the basic plane wave of 700 eV was used. To integrate the Brillouin zone in the inverse space, the Monkhorst-Pack scheme with a density of $4 \times 4 \times 4$ was used. These parameters provided good compliance in total energy. For the calculations, the convergence resistance was chosen as the total energy difference in the range of 10^{-7} eV/atom. The given electronic configurations for pseudopotentials: Mn ($3d^6 4s^1$), Fe ($3d^6 4s^2$), V ($3d^4 4s^1$), Si ($3s^2 3p^2$), respectively.

1. STRUCTURAL PROPERTIES

Heusler alloys with the chemical formula X_2YZ (where X and Y are transition metal atoms, and Z is a valence atom of s-p type) are characterized by a cubic structure similar to Cu_2MnAl , consisting of four interlocking *fcc* sublattices, denoted as A, B, C, and D. The coordinates of these sublattices are (0,0,0), (0.25, 0.25, 0.25), (0.5, 0.5, 0.5), and (0.75, 0.75, 0.75). X atoms are arranged in the same way in sublattices A and C and atoms Y and Z occupied B and D, respectively. The reverse structure of the Heusler alloy also crystallizes with Hg_2CuTi type structure, while Cu_2MnAl is known for the full structure. The main difference from regular Heusler compounds with the L_{21} structure is the mutual exchange between X in position C and Y in position B. Studied structural models are presented in Figure 1.

Generally, the unit cell contains 4 structural units X_2YZ . The location of atoms and their coordinates were discussed in our previous articles [10].

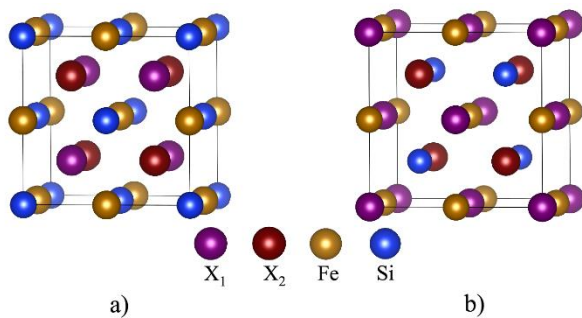


Figure 1. Crystal structure of Heusler compounds.
a) Regular structure (L_{21}) and b) inverse structure (XA).
 $X_2\text{FeSi}$ ($X = \text{Mn}, \text{V}$)

The calculations have shown that all three functions give qualitatively the same energy ratios. For both Mn_2FeSi and V_2FeSi , the energetically more advantageous phase is XA. LDA, GGA and SCAN calculations give ΔH equal to -1.5087 (-1.8907) eV,

-1.3836 (-1.5226) eV, and -1.9829 (-1.6319) eV, respectively, for Mn_2FeSi (V_2FeSi) structures. The calculated enthalpy of formation has a negative value, which indicates the possibility of Mn_2FeSi and V_2FeSi formation in the experiment.

The enthalpy of formation was determined using the formula:

$$\begin{aligned} \Delta H (\text{Mn}_2\text{FeSi} / \text{V}_2\text{FeSi}) &= \\ &= [H (\text{Mn}_2\text{FeSi} / \text{V}_2\text{FeSi}) - \\ &\quad - 2H (\text{Mn}) + H (\text{Fe}) + H (\text{Si})] / N, \end{aligned} \quad (1)$$

where $H(\text{Mn}_2\text{FeSi}/\text{V}_2\text{FeSi})$, $H(\text{Mn})$, $H(\text{Fe})$ and $H(\text{Si})$ are the calculated enthalpies of the Heusler alloy and the elements Mn, Fe and Si, respectively, N is the number of structural units in the unit cell.

In the case V_2FeSi , the L_{21} structure is most favorable in SCAN-based calculations, and for LDA and GGA, this structure is less favorable, whereas in Mn_2FeSi , the inverse structure is lower in energy in all calculations (Table 1). This aligns with the existing experimental data [7].

Table 1. Calculated ground state energies and formation enthalpies of Mn_2FeSi and V_2FeSi

Atoms	Structure	Type of functional	Formation enthalpy H_{cp} (eV/cell)	Energy(eV)
Mn_2FeSi	XA	LDA	-1.5087	-148.4113
Mn_2FeSi	L_{21}	LDA	-1.1648	-147.0356
V_2FeSi	XA	LDA	-1.8907	-147.1947
V_2FeSi	L_{21}	LDA	-1.2529	-144.6431
Mn_2FeSi	XA	GGA	-1.3835	-132.1324
Mn_2FeSi	L_{21}	GGA	-0.9690	-130.4259
V_2FeSi	XA	GGA	-1.5226	-131.5246
V_2FeSi	L_{21}	GGA	-0.7436	-128.4368
Mn_2FeSi	XA	SCAN	-1.9829	-132.4391
Mn_2FeSi	L_{21}	SCAN	-1.3124	-131.0985
V_2FeSi	XA	SCAN	-1.6319	-123.9251
V_2FeSi	L_{21}	SCAN	-1.3275	-128.3164

2. MAGNETIC PROPERTIES

Table 2 displays the equilibrium lattice parameters and magnetic moments of V_2FeSi and Mn_2FeSi in both regular and inverse structures. It is observed that these compounds adopt different structures. The atomic magnetic moment (ASM) values for the various types of atoms in Mn_2FeSi and V_2FeSi Heusler alloys in L_{21} and XA structures are in good agreement with previously reported literature data.

The magnetic properties of the different crystal structures in Mn_2FeSi Heusler alloy are determined by the presence of two types of Mn atoms oriented in the opposite direction of the magnetic moment in the X-type lattice. Table 2 displays the calculated total magnetic moments of the lattices.

Table 2. The lattice parameters (\AA) and total magnetic moments (μ_B) of Mn_2FeSi and V_2FeSi Heusler alloys of regular and inverse structures, as well as magnetic moments (μ_B) of individual atoms, are calculated based on the SCAN, GGA and LDA functionals. In parentheses are the previously calculated theoretical values of the lattice parameter and the total magnetic moments and magnetic moments of individual atoms. Due to the Slater-Pauling rule [25], the total magnetic moment is $2 \mu_B$ for Mn_2FeSi and V_2FeSi .

Compounds	Structure	Type of functional	Lattice parameter	A-site atom μ_B	B-site atom μ_B	C-site atom μ_B	D-site, Si atom μ_B	Total μ_B
Mn_2FeSi	XA	SCAN	5.617 ^(a)	Mn ₁ -2.012 ^(a)	Mn ₂ 2.961 ^(a)	Fe 1.039 ^(a)	0.012 ^(a)	1.99 ^(a)
	L_{21}	SCAN	5.538 ^(a)	Mn ₁ -0.271 ^(a)	Fe 2.495 ^(a)	Mn ₂ -0.271 ^(a)	0.041 ^(a)	1.99 ^(a)
	L_{21}	SCAN	5.54 ^(b)	Mn ₁ -0.32 ^(b)	Fe 2.52 ^(b)	Mn ₂ -0.32 ^(b)		2.00 ^(b)
	L_{21}		5.60 ^(c)	Mn ₁ -0.78 ^(c)	Fe 0.33 ^(c)	Mn ₂ 2.48 ^(c)	-0.02 ^(c)	2.01 ^(c)
	XA	GGA	5.599 ^(a)	Mn ₁ -0.777 ^(a)	Mn ₂ 2.371 ^(a)	Fe 0.365 ^(a)	0.011 ^(a)	1.96 ^(a)
	L_{21}	GGA	5.594 ^(a)	Mn ₁ 0.061 ^(a)	Fe 2.106 ^(a)	Mn ₂ 0.061 ^(a)	0.026 ^(a)	2.25 ^(a)
	XA	LDA	5.477 ^(a)	Mn ₁ -0.346 ^(a)	Mn ₂ 1.999 ^(a)	Fe 0.300 ^(a)	0.008 ^(a)	1.96 ^(a)
	L_{21}	LDA	5.483 ^(a)	Mn ₁ 0.090 ^(a)	Fe 1.807 ^(a)	Mn ₂ 0.090 ^(a)	0.028 ^(a)	2.01 ^(a)
V_2FeSi	XA	SCAN	5.748 ^(a)	V ₁ -0.700 ^(a)	V ₂ 1.721 ^(a)	Fe 1.074 ^(a)	-0.056 ^(a)	2.00 ^(a)
	L_{21}	SCAN	5.805 ^(a)	V ₁ 0.133 ^(a)	Fe 2.081 ^(a)	V ₂ 0.133 ^(a)	0.025 ^(a)	2.37 ^(a)
	L_{21}		5.80 ^(c)	V ₁ 0.45 ^(c)	Fe -0.093 ^(c)		0.05 ^(c)	1.99 ^(c)
	XA	GGA	5.782 ^(a)	V ₁ 1.440 ^(a)	V ₂ -0.331 ^(a)	Fe 0.894 ^(a)	-0.019 ^(a)	1.98 ^(a)
	L_{21}	GGA	5.853 ^(a)	V ₁ 0.081 ^(a)	Fe 2.025 ^(a)	V ₂ 0.081 ^(a)	0.038 ^a	2.22 ^(a)
	XA	LDA	5.748 ^(a)	V ₁ 0.394 ^(a)	V ₂ -0.046 ^(a)	Fe 0.254 ^(a)	-0.001 ^(a)	0.60 ^(a)
	L_{21}	LDA	5.805 ^(a)	V ₁ 0.003 ^(a)	Fe 1.612 ^(a)	V ₂ 0.003 ^a	0.042 ^(a)	1.66 ^(a)

In this work (a) – present work, (b) – theoretical data from Ref. [13], (c) – theoretical data from Ref. [26]

According to the results obtained from the SCAN and GGA-LDA calculations, the total magnetic moment of Mn_2FeSi Heusler alloys with XA and L_{21} structures are presented in Table 2, with values of (1.99, 1.96, 1.96) μ_B and (1.99, 2.25, 2.01) μ_B , respectively. These results follow the Slater-Pauling rule (S-P rule) [22]. However, the LDA calculation shows a slight deviation in the total magnetic moment for the XA type (1.96 μ_B), while GGA shows a deviation for the L_{21} type (2.25 μ_B). The S-P rule suggests that the total magnetic moment in semimetallic full Heusler compounds can be determined by the formula $M_t = Z_t - 24$, where Z_t is the total number of valence electrons per unit cell and M_t is the magnetic moment of the unit cell [22].

When using LDA and GGA functionals, the total magnetic moment values of the L_{21} (1.66 μ_B) and XA (0.60 μ_B) lattices do not comply with the Slater-Pauling rule due to the ferromagnetic coupling of V and Fe atoms. However, based on GGA, the values are L_{21} (2.22 μ_B) and XA (1.98 μ_B), which are consistent with the Slater-Pauling rule. In SCAN calculations, the structure of type XA (2.00 μ_B) completely follows the Slater-Pauling rule, while type L_{21} (2.37 μ_B) has a significant deviation.

The magnetic moments of transition metal atoms differ significantly due to their distinct local environment in both types of structures. In Heusler compounds, the magnetic state primarily depends on the position of metal atoms within the local environment. As stated in references [27, 28], the presence of transition metal atoms as the closest neighbors leads to the formation of strong σ -bonds between d-electrons of these atoms. However, the deviation from d-electron localization leads to a decrease in magnetic moments, which is a characteristic feature of Heusler compounds. Therefore, based on the observations of the magnetic moments of Mn_2FeSi and V_2FeSi Heusler alloys, the atoms at A- and C-positions exhibit smaller magnetic moments, while the

atom at the B-position has a larger magnetic moment in both structural types, which supports the conclusion of references [27, 28].

Figure 2 shows the correspondence of the functionals to the Slater-Pauling rule. Upon analysis of the results, it can be deduced that the functionals utilized for the Mn_2FeSi alloy yielded values in accordance with the Slater-Pauling rule. However, for the L_{21} and XA structures, the LDA and GGA functionals demonstrated deviations from the aforementioned rule. Whereas the SCAN showed more accurate data.

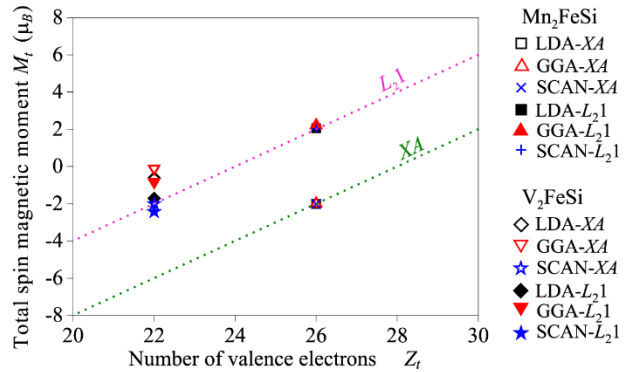


Figure 2. Correspondence of functionals LDA, GGA and SCAN to the Slater-Pauling rule

3. ELECTRONIC PROPERTIES

Figure 3 presents the total state densities (DOS) of Mn_2FeSi and V_2FeSi compounds in full and inverse structures, calculated in GGA approximations (blue line in Figure 3), LDA (dotted line in Figure 3) and SCAN (the red line in Fig. 3). As is known, the approximation of GGA and LDA inaccurately estimates the width of the forbidden zone, significantly underestimating its value. Mn_2FeSi in the regular structure (Figure 3b) are metals within GGA and LDA, whereas calculations based on SCAN adduce to the appearance of a small band gap of

~ 0.4 eV (Figure 3b). In the inverse structure, SCAN increases the band gap from ~ 0.35 eV (within GGA) to ~ 0.65 eV (Figure 3a). In the GGA and LDA approximations, the V_2FeSi compound in both structures ($L2_1$, XA) exhibits a metallic character (Figure 3d). However, SCAN increases the band gap to ~ 0.75 eV in the inverse structure, and the regular structure exhibits a metallic character with an almost empty spin-up channel (Figure 3c).

The obtained values of the band gap for Mn_2FeSi compounds obtained here are close to other results of calculations studied by means of the GGA and SCAN approximation [15]. For instance, in [15] the band gap width was obtained equal to ~ 0.5 eV (within GGA) and ~ 1.0 eV (within SCAN) for the inverse Mn_2FeSi and for the regular $0.2 \sim 0.4$ eV.

Figure 4 shows the partial densities of d-electron states for V_2FeSi and Mn_2FeSi in full and inverse structures. All projected DOS have pronounced peaks corresponding to the strong localization of electrons of B-position atoms.

As can be seen, the appearance of semi-metallic properties in these Heusler compounds is mostly because

of the behavior of t_{2g} electrons of transition metal atoms. In the literature [15] explains the appearance of semimetallic properties of Mn_2FeSi (XA , $L2_1$ structures) with the behavior of t_{2g} electrons of transition metal atoms, where the delocalization of these electrons leads to a strong decrease in the semimetallic band gap. Obtained SCAN calculations are in accord with the results of this literature (Figures 4e, g). Next, we will consider in more detail the predicted density of states of non-basic spin states of t_{2g} electrons of transition metals. Consider the usual connection V_2FeSi (Figure 4a). Atom V in regular V_2FeSi occupies the B-position and has a large magnetic moment and has a local environment: atom V in regular V_2FeSi have Fe as the nearest four atoms (Figure 1a). This local environment leads to a difference in the densities of electronic states, namely, in the regular V_2FeSi , the t_{2g} electrons of V atoms are delocalized in a wider energy range than the t_{2g} electrons of Mn atoms in the regular Mn_2FeSi . As a result, the semi-metallic band gap in the regular V_2FeSi disappears. In the inverse V_2FeSi (Figure 4c), the situation is somewhat different.

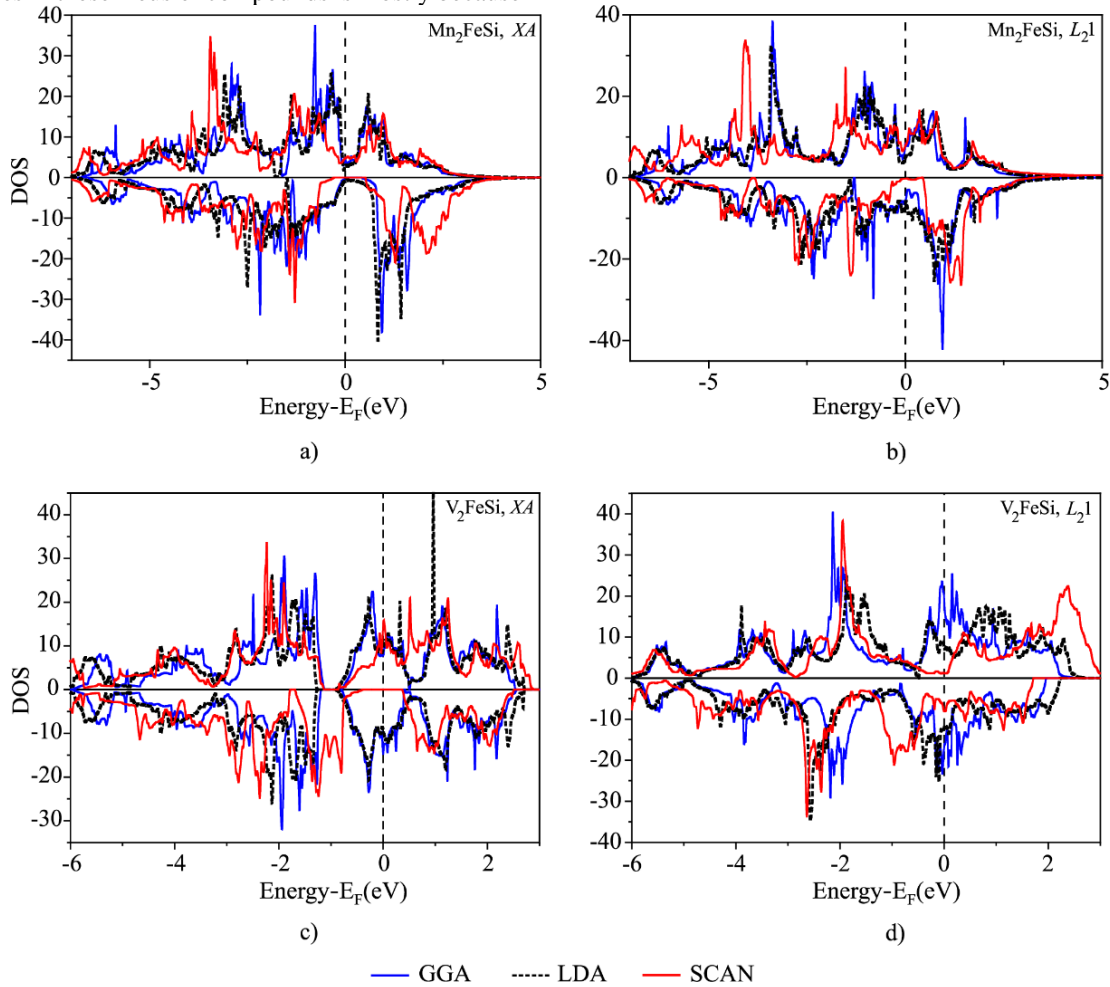


Figure 3. The graphs in (a), (b), (c), and (d) display the total density of states for Mn_2FeSi and V_2FeSi alloys in both full and inverse structures. The red solid line shows results based on the SCAN method, the blue solid line represents GGA, and the dotted line represents LDA. The energy axis is set to zero at the Fermi energy.

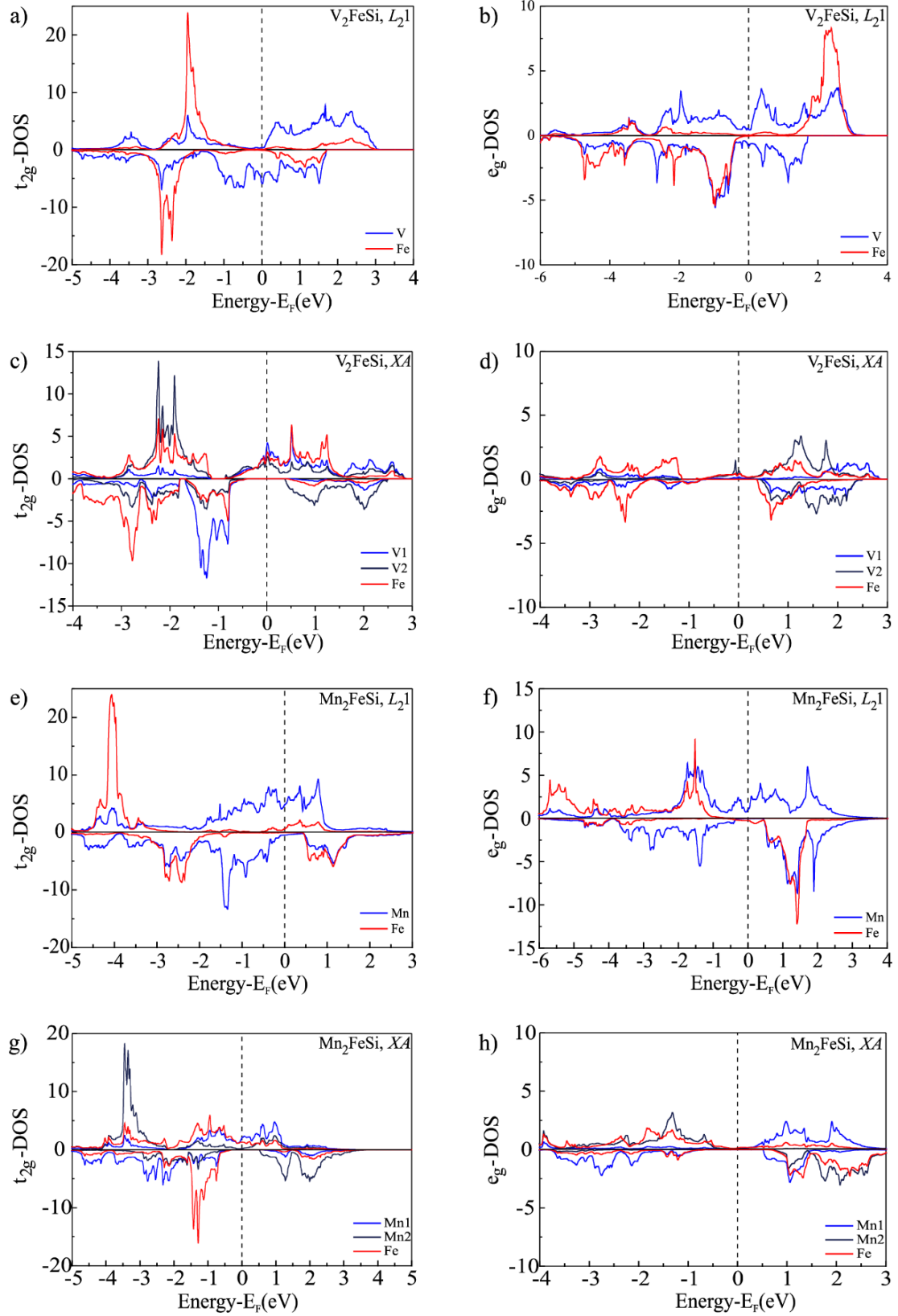


Fig. 4. The density of states of d-electrons for $V_2\text{FeSi}$ in its regular structure (a, b), inverse structure (c, d), $Mn_2\text{FeSi}$ in its regular structure (e, f), and inverse structure (g, h) are shown in the partial density of states. The Fermi energy is at zero on the energy axis.

The Fe atom in this case has the same local environment as in the typical V_2FeSi compound, where it is surrounded by four V atoms that are the closest neighbors. And, as in the regular compound V_2FeSi , the t_{2g} electrons of V atoms are delocalized in a wide range of energies. The shift of the delocalization region of t_{2g} electrons towards lower energies reduces the non-main spin band gap and is associated with strong hybridization of t_{2g} electrons of vanadium atoms. Vanadium atoms V1 and V2 interact only in refers to the nearest neighboring atoms around a particular atom in a crystal structure. Consequently, V2 electrons are localized at energies $\sim -2.2 \div -1.7$ eV and the hybridization of V1 and V2 t_{2g} electrons is observed in the energy range -2.5 eV \div -1.5 eV.

That is, the bonds that appear between metal atoms affect the appearance of a semimetallic band gap. Worth bearing in mind a significant semi-metallic band gap in the alloy V_2FeSi structure XA appears only when the B-position is occupied by a V2 atom with a large magnetic moment. If the B-position is occupied by a manganese atom, then the energy gap in the non-basic spin state in the Mn_2FeSi alloy decreases significantly.

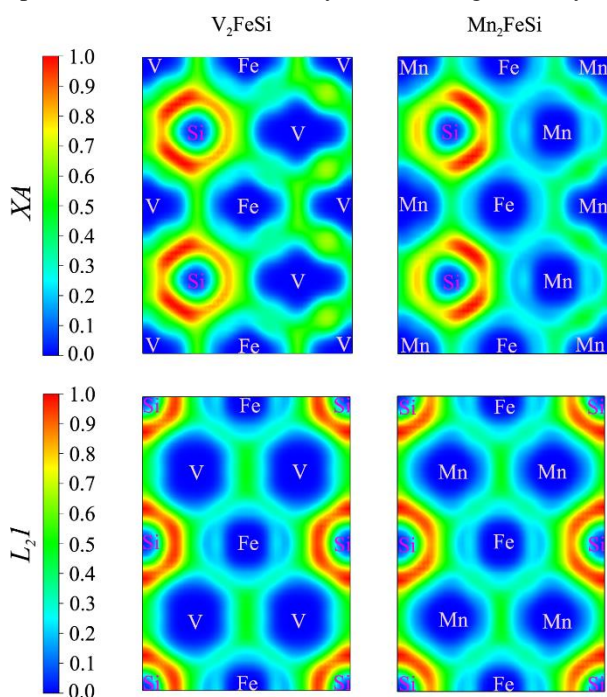


Fig. 5. ELF values were calculated for the L_{21} and XA structures of V_2FeSi and Mn_2FeSi in the (110) plane

Figure 5 presents the ELF projections in the plane (110) for the V_2FeSi and Mn_2FeSi Heusler alloys. In areas where ELF values are high the electrons become paired. In regions with higher ELF values, electrons tend to become paired, this means that in these compounds between atoms, the nature of the bond is covalent. The stability of a compound increases when the covalent bond is strengthened. However, when the degree of polarity of the covalent bond increases, it can compete

with the bond strengthening effect and lead to compound destabilization. In the case of replacing manganese atoms with vanadium in compounds, this effect was observed. High ELF values were observed near V atoms, which indicate the polarity of the covalent bond.

Replacing Mn atoms with V atoms increases the stability of the crystal lattice due to the increased covalence of chemical bonds between atoms in the alloys. However, this substitution also results in a strong polarity of the covalent bond between V atoms and their nearest neighbors, which can destabilize the crystal lattice. As a result, the final crystal compounds are a result of a compromise between these two opposing effects.

CONCLUSION

This study aimed to investigate how the magnetic and electronic properties of Mn_2FeSi and V_2FeSi Heusler alloys are influenced by their structure and composition, particularly by the local environment and the composition and structure of the alloys. The B-position atoms in these alloys have larger magnetic moments than the A- and C-position atoms, which is attributed to differences in their local surroundings. The researchers used three different functionals to calculate the energy stability of the L_{21} and XA structures and found that the XA structure is energetically favorable for both alloys. The meta-GGA functional (SCAN) was the most accurate in describing the electronic properties of the alloys. Both Mn_2FeSi and V_2FeSi were found to be semimetals, with the semimetallic band gap arising from the bonds between neighboring metal atoms. In V_2FeSi , a significant semimetallic band gap is only present in the XA structure when the B-position is occupied by a V2 atom with a large magnetic moment.

The study also showed that the B-position atom in both structural types has a large magnetic moment, while the A and C-position atoms have smaller ones. The total magnetic moment of both Mn_2FeSi and V_2FeSi alloys is consistent with the Slater-Pauling rule, as revealed by the SCAN calculations.

REFERENCES

1. M.N. Rasul, A. Javed, M.A. Khan, A. Hussain, Structural stability, mechanical, electronic and magnetic behavior of quaternary ScNiCrX ($X = \text{Al}, \text{Ga}$) Heusler alloys under pressure, *Mater. Chem. Phys.* 222 (2018) 321–332. <https://doi.org/10.1016/j.matchemphys.2018.09.015>
2. A. Abada, K. Amara, S. Hiadsi, B. Amrani, First principles study of a new halfmetallic ferrimagnets Mn2-based full Heusler compounds: Mn_2ZrSi and Mn_2ZrGe , *J. Magn. Magn. Mater.* 388 (2015) 59–67. <https://doi.org/10.1016/j.jmmm.2015.04.023>
3. Y. Ze-Jin, G. Qing-He, X. Heng-Na, et al., Pressure-induced magnetic moment abnormal increase in Mn_2FeAl and non-continuing decrease in Fe_2MnAl via first principles, *Sci. Rep.* 7 (1) (2017) 16522. <https://doi.org/10.1038/s41598-017-16735-1>
4. S. Qi, C.-H. Zhang, B. Chen, J. Shen, N. Chen, First-principles study on the ferrimagnetic half-metallic

- Mn₂FeAs alloy, *J. Solid State Chem.* 225 (2015) 8–12, <https://doi.org/10.1016/j.jssc.2014.11.026>
5. S. Ahmad Khandy, J.-D. Chai, Novel half-metallic L21 structured full-Heusler compound for promising spintronic applications: a DFT-based computer simulation, *J. Magn. Mater.* (2019) 165289. <https://doi.org/10.1016/j.jmmm.2019.165289>
 6. F.U. Abuova, T.M. Inerbayev, A.U. Abuova, G.A. Kaptagay, N.A. Merali, N. Soltanbek // Electronic structure, magnetic properties and stability of Heusler alloys Mn₂Co_{1-x}V_xZ (Z = Al, Ga). *NNC RK Bulletin.* – 2020. – No. 4(84). – P. 22–29. [in rus.]
 7. Said Bakkar, *New Inverse-Heusler Materials with Potential Spintronics Applications Theses.* 2207, Southern Illinois University Carbondale, United States, 2017, p. 75.
 8. A.B. Granovskii, E.A. Soboleva, Fadeev, et al., Martensitic phase transition in magnetic thin films based on inverse Mn₂FeSi Heusler alloys, *J. Exp. Theor. Phys.* 130 (1) (2020) 117–122. <https://doi.org/10.1134/s1063776119120033>
 9. Sergey V. Faleev, Yari Ferrante, Jaewoo Jeong, Mahesh G. Samant, Barbara Jones, and Stuart S. P. Parkin, Origin of the Tetragonal Ground State of Heusler Compounds, *Phys. Rev.* 7 (3) (2017). <https://doi.org/10.1103/PhysRevApplied.7.034022>
 10. Abuova, F., et al., Structural, Electronic and Magnetic Properties of Mn₂Co_{1-x}V_xZ (Z= Ga, Al) Heusler Alloys: An Insight from DFT Study. *Magnetochemistry*, 2021. 7(12): p. 159.
 11. Abuova, A., et al., Electronic Properties and Chemical Bonding in V₂FeSi and Fe₂VSi Heusler Alloys. *Crystals*, 2022. 12(11): p. 1546.
 12. H. Z. Luo, H. W. Zhang, Z. Y. Zhu, L. Ma, S. F. Xu, G. H. Wu, X. X. Zhu, C. B. Jiang, and H. B. Xu, Half-metallic properties for the Mn₂FeZ (Z=Al, Ga, Si, Ge, Sb) Heusler alloys: A first-principles study, *Journal of Applied Physics* 103, 083908 (2008). <https://doi.org/10.1063/1.2903057>
 13. A. Aryal, S. Bakkar, H. Samassekou, et al., Mn₂FeSi: an antiferromagnetic inverse-Heusler alloy, *J. Alloys Compd.* 823 (2020) 153770, <https://doi.org/10.1016/j.jallcom.2020.153770>
 14. Jianhua Ma, Jiangang He, Dipanjan Mazumdar, et al., Computational investigation of inverse Heusler compounds for spintronics applications, *Phys. Rev. B* 98 (2018), 094410. <https://doi.org/10.1103/PhysRevB.98.094410>
 15. Oksana N. Draganyuk, Vyacheslav S. Zhandun*, Natalia G. Zamkova, Half-metallicity in Fe₂MnSi and Mn₂FeSi Heusler compounds: A comparative ab initio study, *Materials Chemistry and Physics*, Vol. 271, 2021, 124897. <https://doi.org/10.1016/j.matchemphys.2021.124897>
 16. Ondřej Životský, Kateřina Skotnicová, Tomáš Čegan, Jan Juríca, Lucie Gembalová, František Zažímal and Ivo Szurman, Structural and Magnetic Properties of Inverse-Heusler Mn₂FeSi Alloy Powder Prepared by Ball Milling, *Materials (Basel)*. 2022; 15(3): 697. <https://doi.org/10.3390/ma15030697>
 17. M.A. Zagrebin, V.D. Buchelnikov, V.V. Sokolovskiy, I.A. Taranenko, S.I. Saunina, First Principles Calculations of Magnetic Exchange Parameters of Fe-Mn-Al Heusler Alloys. *Solid State Phenomena.* – 2014. – Vol. 215. – P. 131–136. <https://doi.org/10.4028/www.scientific.net/SSP.215.131>
 18. I. Galanakis, K. Özdoğan, E. Şaşıoğlu and B. Aktaş, Doping of Mn₂VAl and Mn₂VSi Heusler alloys as a route to half-metallic antiferromagnetism, *Phys. Rev. B* 75, 092407. <https://doi.org/10.1103/PhysRevB.75.092407>
 19. Blöchl, P. E. Projector augmented-wave method / P. E. Blöchl // *Phys. Rev.* – 1994. – V. 50, No. 24. – P. 17953–17979.
 20. P. Hohenberg and W. Kohn, Inhomogeneous Electron Gas, *Phys. Rev.* 136, B864 (1964). <https://doi.org/10.1103/PhysRev.136.B864>
 21. W. Kohn and L.J. Sham, Self-Consistent Equations Including Exchange and Correlation Effects, *Phys. Rev.* 140, A1133 (1965). <https://doi.org/10.1103/PhysRev.140.A1133>
 22. J.P. Perdew, K. Burke, and M. Ernzerhof, Generalized Gradient Approximation Made Simple, *Phys. Rev. Lett.* 77, 3865 (1996). <https://doi.org/10.1103/PhysRevLett.77.3865>
 23. J. Sun, R.C. Remsing, Y. Zhang, Z. Sun, A. Ruzsinszky, H. Peng, Z. Yang, A. Paul, U. Waghmare, X. Wu, M.L. Klein, and J.P. Perdew, Accurate first-principles structures and energies of diversely bonded systems from an efficient density functional, *Nat. Chem.* 8, 831 (2016). <https://doi.org/10.1038/nchem.2535>
 24. J. Sun, B. Xiao, Y. Fang, R. Haunschild, P. Hao, A. Ruzsinszky, G.I. Csonka, G.E. Scuseria, and J.P. Perdew, Density Functionals that Recognize Covalent, Metallic, and Weak Bonds, *Phys. Rev. Lett.* 111, 106401 (2013). <https://doi.org/10.1103/PhysRevLett.111.106401>
 25. I. Galanakis, P.H. Dederichs, N. Papanikolaou, Slater-Pauling behavior and origin of the half-metallicity of the full-Heusler alloys, *Phys. Rev. B* 66 (2002) 174429.
 26. S. Skafrouros, K. Özdoğan, E. Şaşıoğlu, and I. Galanakis, Generalized Slater-Pauling rule for the inverse Heusler compounds, *Phys. Rev. B* 87, 024420. <https://doi.org/10.1103/PhysRevB.87.024420>
 27. N.G. Zamkova, V.S. Zhandun, S.G. Ovchinnikov, I.S. Sandalov, Effect of local environment on moment formation in iron silicides, *J. Alloys Compd.* 695 (2017) 1213–1222.
 28. F.U. Abuova, T.M. Inerbaev, A.U. Abuova, G.A. Kaptagay, N.A. Merali, Structural, electronic and magnetic properties of vanadium doped Mn₂CoZ(Al/Ga). *News of the Academy of Sciences of the Republic of Kazakhstan. al-Farabi Kazakh National University.* 5 (339), 2021 [in rus.]. <https://doi.org/10.32014/2021.2518-1726.79>

$X_2\text{FeSi}$ ГЕЙСЛЕР ҚОРЫТПАЛАРЫН АЛҒАШҚЫ ПРИНЦИПТЕРДЕН ЗЕРТТЕУ**Н. А. Мерәлі¹, Н. С. Солтанбек¹, Ф. У. Абуова¹, Т. М. Инербаев^{1,2}, С. А. Нуркенов^{1,3}, А. У. Абуова^{1*}**¹ «Л.Н. Гумилев атындағы Еуразия ұлттық университеті» КеАҚ, Астана, Қазақстан² Геология және минералогия институты. Соболева РАН, Новосибирск, Ресей³ Астана Халықаралық Университеті, Астана, Қазақстан

* Байланыс үшін E-mail: aisulu-us1980@yandex.kz

Тығыздық функционалы теориясының аясында $X_2\text{FeSi}$ ($X = \text{Mn}, \text{V}$) толық (L_{21}) және кері (XA) Гейслер қорытпаларының электрондық және магниттік қасиеттері зерттелді. Есептеулер үш түрлі функционалмен, LDA, GGA және meta-GGA, жүргізілді. Зерттеу жұмысында L_{21} және XA құрылымдары үшін энергетикалық тұрақтылығы жоғары құрылымды анықтау. Алынған мәліметтерден екі құрылым үшін де энергетикалық тұрақты екенін XA құрылымы көрсетті. Функционалды таңдау фазалардың энергетикалық тұрақтылығына әсер етпейтіні анықталды. Есептеулер негізінде meta-GGA (SCAN) қорытпалардың электрондық қасиеттерін дәлірек сипаттайтыны анықталды. Есептеулер барысында бұл қорытпалар жартылай металл екені анықталды. Гейслер қорытпаларының жартылай металл пайда болатын тыйым салынған аймақтың және электрондық және магниттік қасиеттердің өзгеруінің себептерін зерттеу және түсіну үшін локальді орта тұрғысынан талдау жүргізілді. Есептеулер сонымен қатар екі құрылым үшін Mn_2FeSi магниттік моменті $1,99 \mu_B/\text{ф.б.}$ екенін көрсетті. V_2FeSi үшін. XA құрылымында $\mu = 2,00 \mu_B/\text{ф.б.}$ және L_{21} құрылымында $\mu = 2,37 \mu_B/\text{ф.б.}$ Бұл есептеулер XA құрылымына арналған Слейтер-Полинг ережесіне сәйкес келеді.

Түйін сөздер: Гейслер қорытпалары, тығыздық функционалдық теориясы, магниттік қасиеттер.

ПЕРВОПРИНЦИПНЫЕ ИССЛЕДОВАНИЯ СПЛАВОВ ГЕЙСЛЕРА $X_2\text{FeSi}$ **Н. А. Мерали¹, Н. С. Солтанбек¹, Ф. У. Абуова¹, Т. М. Инербаев^{1,2}, С. А. Нуркенов^{1,3}, А. У. Абуова^{1*}**¹ НАО «Евразийский национальный университет им. Л.Н. Гумилева», Астана, Казахстан² Институт геологии и минералогии им. Соболева РАН, Новосибирск, Россия³ Астанинский международный университет, Астана, Казахстан

* E-mail для контактов: aisulu-us1980@yandex.kz

В рамках теории функционала плотности изучены характеристики, связанные с электричеством и магнетизмом в сплавах Гейслера как с полной (L_{21}), так и с инверсной (XA) структурой $X_2\text{FeSi}$ ($X = \text{Mn}, \text{V}$). Расчеты проводились на трех различных функционалах: LDA, GGA и meta-GGA. Цель состояла в том, чтобы исследовать энергетическую стабильность структур L_{21} и XA для этих композиций. Полученные данные показали, что структура XA является энергетически стабильной для обеих структур. Отмечено, что выбор функционала не оказывает качественного влияния на энергетическую устойчивость фаз. На основе расчетов было установлено, что meta-GGA (SCAN) более точно описывает электронные свойства этих сплавов. В процессе расчетов было установлено, что эти соединения являются полуметаллами. Был проведен анализ с точки зрения местной окружающей среды, чтобы исследовать и понять причины полуметаллической запрещенной зоны и изменения электронных и магнитных свойств, наблюдаемые в соединениях Гейслера. Расчеты также показали, что магнитный момент Mn_2FeSi для обеих структур составляет $1,99 \mu_B/\text{ф.е.}$ Для V_2FeSi $\mu = 2,00 \mu_B/\text{ф.е.}$ для структуры XA и $\mu = 2,37 \mu_B/\text{ф.е.}$ для структуры L_{21} . Эти расчеты согласуются с правилом Слейтера-Полинга для XA -структуры.

Ключевые слова: сплавы Гейслера, теория функционала плотности, магнитные свойства.